arXiv:cond-mat/0602207v1 [cond-mat.dis-nn] 8 Feb 2006

Link between the diversity, heterogeneity and kinetic properties of amorphous ice structures

M. M. Koza, T. Hansen, R. P. May, H. Schober

Institut Laue–Langevin, 6 rue Jules Horowitz, F–38042 Grenoble Cedex 9, France.

Abstract

Based on neutron wide–angle diffraction and small–angle neutron scattering experiments, we show that there is a correlation between the preparational conditions of amorphous ice structures, their microscopic structural properties, the extent of heterogeneities on a mesoscopic spatial scale and the transformation kinetics. There are only two modifications that can be identified as homogeneous disordered structures, namely the very high–density vHDA and the low–density amorphous LDA ice. Structures showing an intermediate static structure factor with respect to vHDA and LDA are heterogeneous phases. This holds independently from their preparation procedure, i.e. either obtained by pressure amorphisation of ice I_h or by heating of vHDA. The degree of heterogeneity can be progressively suppressed when higher pressures and temperatures are applied for the sample preparation. In accordance with the suppressed heterogeneity the maximum of the static structure factor displays a pronounced narrowing of the first strong peak, shifting towards higher Q–numbers. Moreover, the less heterogeneous the obtained structures are the slower is the transformation kinetics from the high–density modifications into LDA. The well known high–density amorphous structure HDA does not constitute any particular state of the amorphous water network. It is formed due to the preparational procedure working in liquid nitrogen as thermal bath, i.e. at about 77 K.

Key words: Amorphous polymorphism, ice, neutron scattering

PACS: 61.12.-q, 61.43.Fs, 64.60.My, 64.70.Kb

1 Introduction

Amorphous polymorphism is a property of solid water well established by experiments. A metastable high–density amorphous structure (HDA, $\rho \approx$ 38 molec./nm^3) can be formed by pressure amorphisation of hexagonal ice I_h at 77 K [1]. HDA transforms upon heating at ambient pressure to a low–density amorphous modification (LDA, $\rho \approx 31$ molec./nm^3). If higher temperatures are applied during the pressure amorphisation of ice I_h or if the formed HDA is subject to a heat treatment at high pressures amorphous structures of higher densities are formed [2,3]. A very high–density structure (vHDA, $\rho \approx 41$ molec./nm^3 has been conjectured to be a third 'state' of amorphous ice [3]. The number of next neighbours has been proposed as a discrimination criterion between the amorphous 'states' LDA, HDA and vHDA from neutron diffraction experiments [4].

The assignment of states to the amorphous ice structures becomes less evident, when transformation properties between the structures are monitored. For example, it has been shown that an HDA sample transforming upon heating into LDA displays a continuum of intermediate static structure factors [5,6,7] and dymanic properties [5,8]. The transformation of vHDA into LDA passes through a structure displaying a structure factor apparently comparable to the one of HDA which, however, does not feature any distinguished properties among other intermediate structures [8].

As far as diffraction experiments are concerned, the evolution of a small–angle neutron scattering (SANS) signal represents rather a counter evidence against the scenario of a multiple of amorphous states. When HDA and vHDA transform into LDA a transient excess in the SANS signal marks the intermediate transformation stages as heterogeneous structures [5,8]. Fingerprints of pronounced heterogeneity can be already observed in HDA samples and only vHDA and LDA proved to be homogeneous and, hence, good candidates for distinguished states [8,9]. The properties of the wide-angle diffraction (WAD) signal indicate that spatial correlations are notedly confined in the intermediate structures, and the evolution of the spatial confinement compares well with the time dependence of the SANS intensity.

In this paper we intensify our studies of the significance of preparation conditions on the WAD and SANS properties. We show that the static structure factor $I(Q)$ of the amorphous ice structures shows a systematic dependence in the sense that the first structure peak shifts towards higher momentum numbers and becomes narrower if higher pressures and/or temperatures are applied. In accordance with the narrowing of the peak, which could be interpreted as an increment of correlations in the amorphous structure, the excess intensity in the SANS signal is reduced, marking the structure as less heterogeneous.

In situ observation of structural changes $I(t, T)$ reveals a progressive slowing down of transformation kinetics for samples prepared at higher temperatures and pressures. Regardless of the applied preparation conditions all samples show comparable structural properties when transforming into LDA. The average size of mesoscopic domains leading to the structure of strongest heterogeneity (SSH) is estimated to about 12 Å.

2 Experimental

Six samples (D_2O, purity of 99.8%) were prepared by pressure amorphisation of ice I_h at $T \approx 77$ K. The maximum pressure of 18 kbars was applied for 10 min. before a lower pressure p_{anneal} was established at which the samples were annealed at T_{anneal} for 30 min. each. After the annealing process all samples were cooled back to 77 K and recovered from the pressure device. An overview of the sample preparation conditions is given in table 1. In addition, a seventh sample was obtained directly by pressure amorphisation at $T \approx 120$ K with a maximum pressure of 15 kbar. It had been equally kept for 30 min. at these conditions before it was recovered at 77 K. The temperature and pressure stability was ± 2 K and ± 0.25 kbar, respectively.

Each of the preparation runs resulted in about 3 ml of sample substance. Each sample was separated into 5–6 portions and used for different experiments, either at different instruments or at the same instrument but at different experimental conditions. The experiments were performed at the wide–angle diffractometer D20 and the small–angle diffractometer D22 at the Institut Laue–Langevin, Grenoble, France. The incident neutron wavelengths used were 2.4 Å and 6.0 Å, respectively. In all measurements standard cryostats were utilised with a He–atmosphere of 200 mbars. The *in situ* experiments and the data treatment were performed in full analogy to the measurements described in detail in references [7,8]. Two temperatures were chosen to follow the structural transformation of the samples *in situ*, namely 108 K and 113 K. All measurements were finished with the LDA structure annealed for 30 min. at 130 K.

To compare all results on a relative scale all WAD data were normalized with respect to the coherent scattering power of LDA. In addition, to compare with SANS data the results have been shifted to give zero scattering towards small scattering angles.

3 Results and Discussion

In Fig. 1 we present exemplary static structure factors of samples #1–#5. Depicted are results from the 'as recovered' states, from stages of transformation comparable to the HDA structure, from the structures of strongest heterogeneity (SSH), and from LDA. It is obvious that beyond the differences of the 'as recovered' structures there is a common behaviour among all samples when transforming into LDA. Besides the well reported evolution of the predominant maximum that shifts progressively towards lower scattering angles [7], and takes on temporarily the lowest intensity and largest width in the middle of the transformation, there is a transient excess intensity in the small–angle part of the diffractograms. The regime of the changing SANS signal is highlighted by the grey area.

There are two important points to be taken note of in the properties of the SANS signal. First of all, its intensity reaches a maximum right in the middle of the transformation and marks this stage as a structure of strongest heterogeneity (SSH). This SSH matches well with the stage at which the structure factor maximum is characterised by the largest width and lowest intensity, as it is reported in [8]. These properties are independent of the sample preparation conditions.

The second important point concerns the 'as recovered' structures, i.e. properties that depend on sample preparation details. As can be seen from the 'as recovered' data in Fig. 1 only samples #4 and #5 display below 30 degs. a flat scattering characteristic, without any excess intensity. In samples #1–#3 an upturn of the signal towards low scattering angles indicates the presence of heterogeneities. To substantiate this point, Fig. 2 a reports the WAD data in comparison with the SANS results in Fig. 2 b taken on different portions of the same samples. Please note, that the SANS response of sample #4 matches the signal of #5 and has been therefore suppressed in Fig. 2 b. There is an obvious and unequivocal correlation between the excess intensity in the SANS data and the position and width of the maximum in the WAD data, respectively. We may conclude that the higher the temperature and/or the higher the pressure during the sample preparation is, the less is the SANS excess intensity, the narrower is the static structure maximum and the higher is its position in the diffractogram.

In other words, only when extreme conditions for the formation of the amorphous ice structures are applied homogeneous samples can be obtained. HDA, as sample #1, and samples #2, and #3 are structurally heterogeneous. To stress the relation between the signal at low–scattering angles and the width of the static structure factor peak, table 2 reports data on the intensity added up as $I_{\mathrm{sas}} = \sum_{0.2\mathring{A}^{-1}}^{0.6\mathring{A}^{-1}} I(Q)$ and the full width at half maximum (FWHM) obtained from a Lorentzian fit to the peak. Not only the I_{sas} and FWHM of samples #1–#5 follow a common trend, but also samples #6 and #7 fit into this picture. The inset in Fig. 2 a reports the peak in $I(Q)$ of #6 and #7 indicating the ressemblance with #2 and #3. As it is demonstrated by the properties of sample #7, pressure amorphisation at higher temperatures than

77 K leads to structures that are less heterogeneous than HDA, however, still displaying an enhanced SANS signal and a clearly broadened peak in the static structure factor.

It is important to note that a recent publication of static structure factors of amorphous ice modifications which have been formed by compression at $T = 125$ K reports an ascending signal towards smaller scattering angles, i.e., smaller Q–numbers for the intermediate structure only [17]. The intermediate structure is denoted as *sample B* in the publication. The recorded small–angle signal is reminiscent of published structure factors from X-ray scattering experiments [9]. It is therefore reasonable to conclude that *sample B* is equally of heterogeneous character.

In order to extract a measure of the extent of the heterogeneous domains we have approximated the SANS signal of the samples in their SSH with the Debye–Bueche model (DBM) [10]. The DBM describes a mixture of two statistically distributed phases leading to the SANS formfactor $I(Q) = I_\circ/(1 + (Q \cdot \gamma)^2)^2$. The correlation length γ takes on the simple relation $2\gamma = D$ with the average domain size D when the occupation numbers of both phases is 50 %, and, thus, the sample in the SSH stage. Examplary fits are depicted in the inset of Fig. 2 b. The data sets have been shifted for clarity. Throughout all the monitored SSH we arrive at a D of 11–13 Å. Within the DBM this small number indicates that structural correlations are confined in the SSH to a space smaller than they are in the homogeneous states, i.e. vHDA and LDA. This result is in full agreement with the extended spatial correlations of vHDA and LDA in comparison to SSH and HDA [8,11]. The absolute value of D corresponds amazingly well with the cutoff distance above which no oscillations are observed in real space distribution functions of SSH [8]. As a clear

consequence, sample properties that are essentially determined by the correlation length are altered progressively by the 'heterogeneous' confinement. For example, the WAD signal of the intermediate structures will not be characterisable by a superposition of the homogeneous structures vHDA and LDA. Hence, the behaviour of the static structure factors does not allow to draw any conclusion upon the nature of the phase transitions between the amorphous ice modifications.

Finally we address the transformation kinetics of the different amorphous ice structures into LDA. We visualize the kinetics in Fig. 3 by the function $I(t,T)$, which has been discussed in detail in [7]. $I(t,T)$ takes on the value 1 for the initial transformation stages, i.e. the 'as recovered' structures. The final LDA states are characterised by 0. Due to the strong variation in kinetic properties of the samples we had to follow the transformations at two different temperatures, whereby two portions of sample #3 served as reference at both T. They are marked as #3/1 and #3/2. Please note that small steps at the end of each data set are due to the annealing of the samples into the LDA structure at $T = 130$ K.

We may easily conclude from the systematic shift of the characteristic transformation times that the less heterogeneous a sample appears to be, the slower is its kinetics when transforming into LDA. This dependence can be intuitively conjectured, on the one hand, from the Adam–Gibbs theory, which predicts that relaxation times are slowed down for systems with lower configurational entropy [12]. The excess SANS intensity of, at least, samples #1 (HDA), #2 and #3 indicates an entropy elevated above that of samples #4 and #5. However, so far it is not clarified whether we deal in the case of the amorphous ice structures with glassy modifications of liquid water to which the Adam–Gibbs

approach might be applicable. There is indeed a number of computer studies questioning the link between the amorphous polymorphism of ice with the liquid state of water [13,14].

On the other hand, if we consistently interprete the amorphous structures in a two–phase scenario, which finds some justification by their heterogeneous character, different initial mixing ratios of two homogeneous phases might equally lead to distinctly different transformation kinetics. This should hold for a transformation comprising strong volume changes as it is the case here [15].

4 Conclusions

We have shown that only the application of extreme conditions in terms of pressure and temperature for the preparation of amorphous ice structures lead to samples which are homogeneous. There is a number of indicators for the grade of sample homogeneity accessible in diffraction experiments. These are, for example, the excess scattering intensity in the small–angle regime, the position and width of the strong maximum in the static structure factor, and the characteristic transformation times in *in situ* studies.

The properties of the SANS intensity offer the opportunity of discriminating between distinguished 'states' of a substance, which are expected to be homogeneous. Only the structures LDA and the sample #5, fullfill this criteria. However, please note that the best homogeneous structure, i.e. the best candidate for a 'state', is not known. The well known modification HDA is a heterogeneous structure and, hence, not a 'state'. Its apparent distinctiveness

is only due to the convenient application of liquid nitrogen for thermalisation of the sample during its preparation.

There is a clear correlation between the grade of heterogeneity of a structure and the properties of its wide–angle diffraction response. As a consequence, the interpretation of the intermediate structures comprising also HDA in real space is not a straightforward procedure. The excess SANS signal should, however, help to discern between different models trying to account for their properties.

The problem of characterising the static properties of the intermediate structures in real space can be well compared with the problem of finding the origin of the non–exponential time response of relaxiations in glasses. There is still no general perception on whether the non–exponential ensemble–averaged time response, is due to a homogeneous or heterogeneous distribution of energy barriers determining the relaxation processes [16]. It is obvious that in the heterogeneous case there is no general way of characterising the system in a unified manner since each sub–ensemble experiences a different relaxation scenario. In fact, the present and previous findings on the small–angle signal [5,8,9] demonstrate that the heterogeneous scenario is applicable in the case of the intermediate amorphous ice structures. Thus, real space distribution functions obtained as Fourier–transforms of the ensemble–averaged static structure factor do not comprise the complexity of the real space structure correctly. The use of only three radial distribution functions to describe the correlations between Oxygens, Hydrogens and cross–terms might be only justified for the LDA and vHDA as homogeneous structures, hence, if the ensemble–averaged static structure factor resembles the characteristics of each of the sub–ensembles.

Finally, results which can be extracted in absolute units from the presented data must not be mistaken as the consequence of the annealing pressure and temperature only, which were applied during the sample formation. Experimental parameters like the compression rate, the annealing time, the decompression procedure, purity grade of the sample substance, etc. may have a well noticeable influence on the sample properties. The experiments reported here were done in a consistent way within one week only including sample preparation and the entire sets of measurements. They should give therefore an accurate qualitative description of the amorphous ice sample properties.

References

[1] O. Mishima, L.D. Calvert and E. Whalley, *Nature*, **310**, 393 (1984).

[2] O. Mishima, *Nature*, **384**, 546, (1996).

[3] T. Loerting, C. Salzmann, I. Kohl, E. Mayer, and A. Hallbrucker, *Phys. Chem. Chem. Phys.*, **3**, 5355, (2001).

[4] J.L. Finney, A. Hallbrucker, I. Kohl, A.K. Soper, and D.T. Bowron, *Phys. Rev. Lett.*, **88**, 225503, (2002); J.L. Finney, D.T. Bowron, A.K. Soper, T. Loerting, and E. Mayer, and A. Hallbrucker. *Phys. Rev. Lett.*, **89**, 205503, (2002).

[5] H. Schober, M. Koza, A. Tölle, F. Fujara, C.A. Angell and R. Böhmer, *Physica* **B**, **241–243**, 897, (1998).

[6] C.A. Tulk, C.J. Benmore, J. Urquidi, D.D. Klug, J. Neuefeind, B. Tomberli and P.A. Egelstaff, *Science*, **297**, 1320, (2002).

[7] M.M. Koza, H. Schober, H.E. Fischer, T. Hansen, and F. Fujara, *J. Phys.: Condens. Matter*, **15**, 321, (2003).

[8] M.M. Koza, B. Geil, K. Winkel, C. Köhler, F. Czeschka, M. Scheuermann, H. Schober, and T. Hansen, *Phys. Rev. Lett.*, **94**, 125506, (2005).

[9] H. Schober, M.M. Koza, A. Tölle, C. Masciovecchio, F. Sette and F. Fujara, *Phys. Rev. Lett.*, **85**, 4100, (2000).

[10] P. Debye and A. M. Bueche, *J. Appl. Phys.*, **20**, 518, (1949).

[11] M. Guthrie, C.A. Tulk, C.J. Benmore, and D.D. Klug, *Chem. Phys. Lett.*, **397**, 335, (2004).

[12] G. Adam and J.H. Gibbs, *J. Chem. Phys.*, **43**, 139, (1965).

[13] V.P. Shpakov, P.M. Rodger, J.S. Tse, D.D. klug, and V.R. Belosludov, *Phys. Rev. Lett.*, **88**, 155502, (2002).

[14] N. Giovambattista, H.E. Stanley, and F. Sciortino, *Phys. Rev. Lett.*, **91**, 115504, (2003).

[15] H. Tanaka, *Europhys. Lett.* **50**, 340, (2000).

[16] N. Giovambattista, M.G. Mazza, S.V. Buldyrev, F.W. Starr, and H.E. Stanley, *J. Phys. Chem. B*, **108**, 6655, (2004).

[17] T. Loerting, W. Schustereder, K. Winkel, C. Salzmann, I. Kohl, and E. Mayer, *Phys. Rev. Lett.*, **96**, 025702, (2006).

Table 1

Sample designation according to the nominal annealing temperature T_{anneal} and annealing pressure p_{anneal}. Please note that sample #7 was first heated to 120 K before having been compressed to 15 kbars. All other samples were first compressed at 77 K before having applied T_{anneal}.

	#1	#2	#3	#4	#5	#6	#7
T_{anneal}/K	77	100	120	140	150	140	120
p_{anneal}/kbar	15	15	15	15	15	12	15

Table 2

Summed intensity in the small–angle regime $I_{\rm sas}$ from the WAD data on the 'as recovered' samples, FWHM and position P of the strong maximum from Lorentzian fits to the WAD signal.

	#1	#2	#3	#4	#5	#6	#7
$I_{\rm sas}$	1.51(8)	0.64(8)	0.35(6)	0.05(6)	0.08(5)	-0.07(9)	0.51(5)
FWHM/Å^{-1}	0.558	0.452	0.406	0.355	0.326	0.361	0.400
P/Å^{-1}	2.120	2.232	2.278	2.316	2.337	2.301	2.271

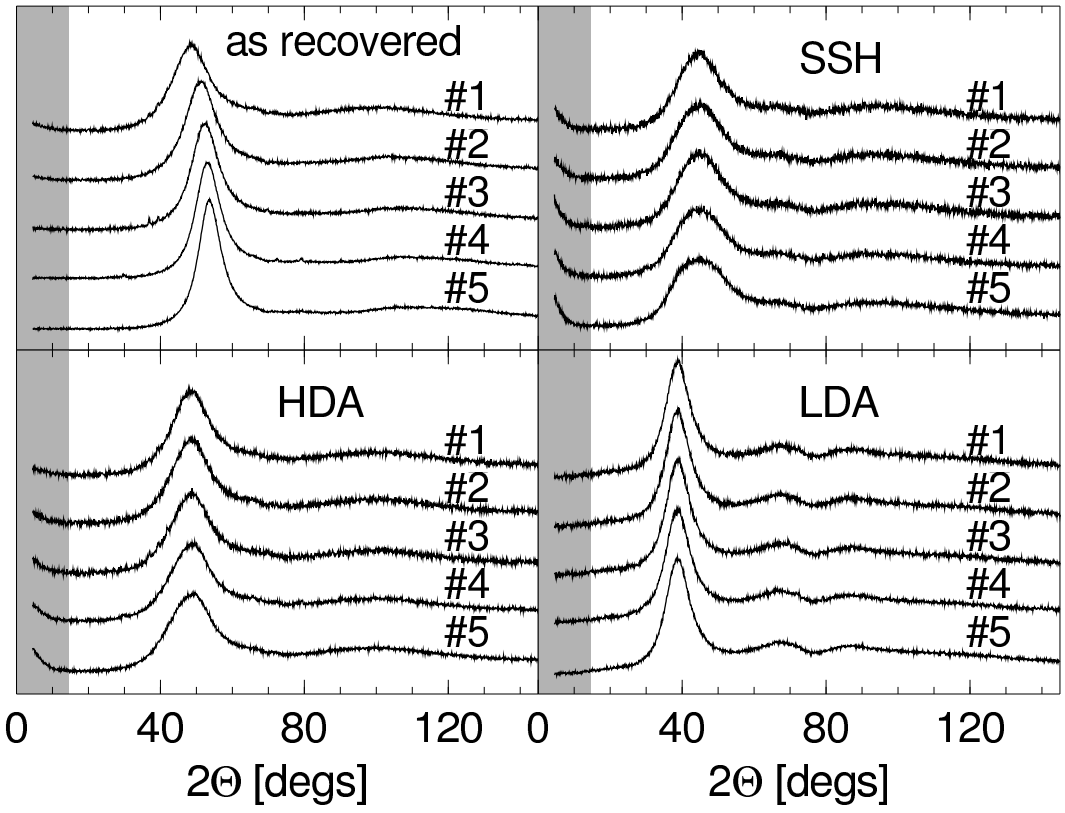


Fig. 1. Static structure factor of samples #1, #2, #3, #4 and #5 as they are recovered, obtained after a certain time in a state comparable with HDA and SSH, and after they were annealed into the LDA structure. The respective data sets have been shifted for clarity.

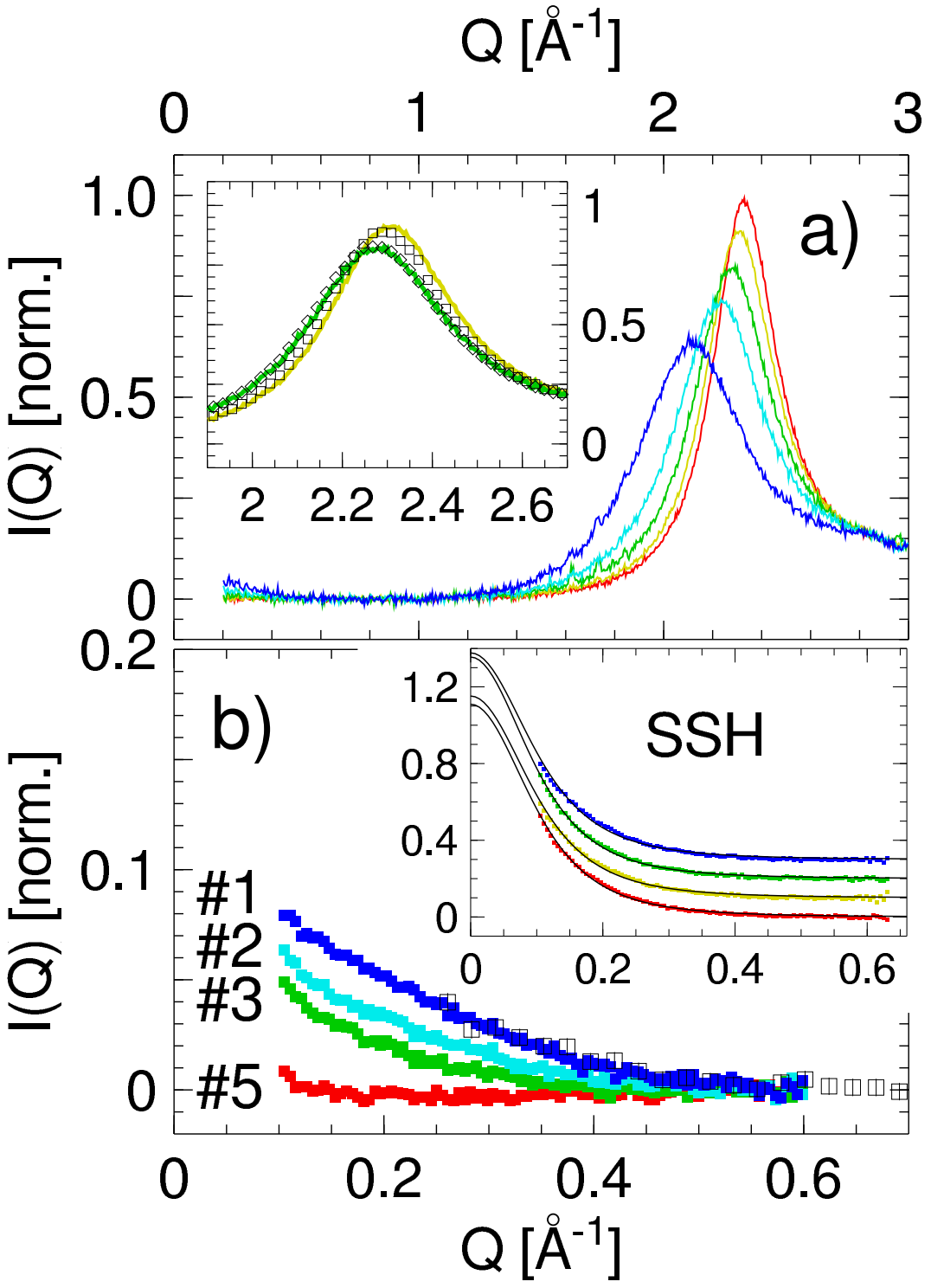


Fig. 2. Figure a: WAD signal of the 'as recovered' samples. The samples correspond from left to right of the maximum position #1 (blue), #2 (cyan), #3 (green), #4 (yellow) and #5 (red). The inset indicates the resemblance of samples #6 (open squares) and #7 (open diamonds) with #4 and #3, respectively. Figure b: SANS signal of the 'as recovered' samples indicated in the figure. Open squares show for comparison data of sample #1 from the D20 measurement. The inset reports the SSH signal and the DRM fit results, explained in the text. The size of data points

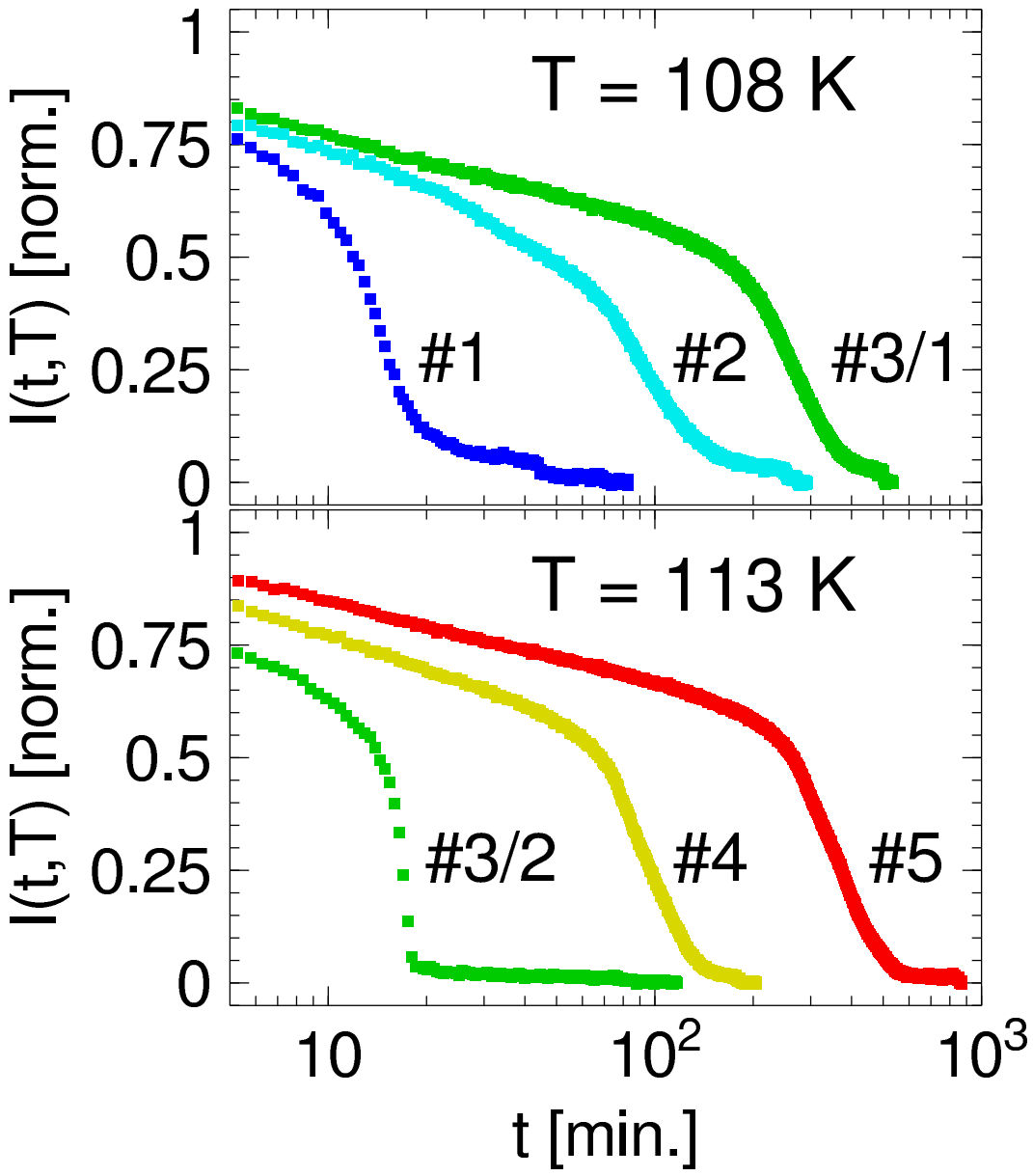


Fig. 3. Transformation kinetics of samples #1–#5 into the LDA modification measured at two different temperatures. Two portions of sample #3 are applied as reference at both temperatures.